AIDA-2020-D9.7

AIDA-2020

Advanced European Infrastructures for Detectors at Accelerators

Deliverable Report

Standard procedures for characterization and qualification

G, Viehhauser (UOXF)

14 April 2020

The AIDA-2020 Advanced European Infrastructures for Detectors at Accelerators project has received funding from the European Union's Horizon 2020 Research and Innovation programme under Grant Agreement no. 654168.

This work is part of AIDA-2020 Work Package **9: New support structures and micro-channel cooling**.

The electronic version of this AIDA-2020 Publication is available via the AIDA-2020 web site <http://aida2020.web.cern.ch> or on the CERN Document Server at the following URL: <http://cds.cern.ch/search?p=AIDA-2020-D9.7>

Grant Agreement No: 654168

AIDA-2020

Advanced European Infrastructures for Detectors at Accelerators

Horizon 2020 Research Infrastructures project AIDA-2020

DELIVERABLE REPORT

STANDARD PROCEDURES FOR CHARACTERIZATION AND QUALIFICATION

DELIVERABLE: D9.7

Document identifier:	AIDA-2020-D9.7
Due date of deliverable:	End of Month 58 (February 2020)
Report release date:	14/04/2020
Work package:	WP9: New support structures and micro-channel cooling
Lead beneficiary:	UOXF
Document status:	Final

Abstract:

This report outlines standard procedures for the qualification and characterization of support structures for vertex and tracking detectors. It first discusses definition of performance-relevant parameters. We will then describe the setups used, and present the testing procedures and support conditions. Aspects of standardization will be discussed. Finally, we will discuss extrapolation of the results to different loads and real operating conditions.

The Advanced European Infrastructures for Detectors at Accelerators (AIDA-2020) project has received funding from the European Union's Horizon 2020 Research and Innovation programme under Grant Agreement no. 654168. AIDA-2020 began in May 2015 and will run for 4 years.

Delivery Slip

	Name	Partner	Date
Authored by	G. Viehhauser	UOXF	25/03/2020
Edited by	P. Giacomelli	INFN	31/03/2020
Reviewed by	A. Reichold P. Petagna M. Vos	UOXF CERN CSIC	27/03/2020 29/03/2020 30/03/2020
Approved by	P. Giacomelli [Deputy Scientific coordinator] Steering Committee		14/04/2020

TABLE OF CONTENTS

EXECUTIVE SUMMARY

This report outlines standard procedures for the qualification and characterization of support structures for vertex and tracking detectors.

1. INTRODUCTION

The purpose of the structure characterization facility at the University of Oxford is to develop techniques to study the deformation of support structures for vertex and tracking systems under representative loads, and thus to support the optimization of such structures, in particular in the reduction of material.

The key requirement for these structures is position stability at the level of a few microns during regular data taking over timescales up to the order of one day. This allows for the reconstruction of the actual position during this period through track-based alignment, and therefore the absolute positioning accuracy for the sense elements is less of a concern.

Over such timescales the relevant loads on the structures are vibration and temperature variations. External vibrations load the structure with an acceleration that can be characterized by a frequency dependent acceleration spectral density (ASD). The ASD is specific to the environment of the tracker. The displacement response is then given by the integral of the convolution of the ASD with the structure response function. External vibration levels in tracking detectors are typically low ($<10^{-7}$ g^2/Hz) due to the static nature of the experiments [1].

The most common source of internal vibrations is coolant flow, in particular in air flow cooling systems due to the fast and turbulent flow. Here, prediction of the displacement response is much more difficult, as it depends on local parameters and geometry of the flow, and consequently standardization of performance measurements and extrapolation to final performance will be more challenging.

Temperature variations can be caused by global changes of the environment, but more often stem from variations of the front-end power, for example due to varying event rates, or the coolant temperature. Such changes will typically lead to non-uniform temperature variations depending on the specific geometry.

2. OVERVIEW OF SETUPS

2.1. VIBRATION SETUP

2.1.1. Setup description

The goal of the vibration setup (`shaker table') at the University of Oxford is the displacement measurement of lightweight structures at very low levels of vibration, providing flexibility in the size and shape of the structure. For this purpose a lightweight carbon-fibre support table has been constructed which is pivoting along one edge and excited by solenoid at one point. The solenoid is driven by the signal from an Arbitrary Waveform Generator (AWG), amplified by an audio power amplifier.

High-sensitivity MEMS accelerometers (LIS344ALH) measure the vibration levels. Displacements are measured using several capacitive distance sensors (capaNCDT 6100 with CS1 sensors), which provide very precise contactless measurements (we have measured sensible displacement amplitudes down to 10 nm). A drawback of this technology is that the

sensors are relatively large (10 mm diameter) and need to be located within a limited range (1 mm) from the surface to be surveyed, which is not a severe limitation for this measurement.

2.1.2. Supports

A critical element for the structural performance is the mechanical interface of the detector structure (ladder, disk, etc.) to the global structure. Ideally, the tests would use a realistic representation of a final design. However, for most of the structures studied at the facility so far this interface has not yet been designed, or has not yet been available. In absence of these final interfaces we have adopted a simple and flexible universal approach. All tested ladder structures had some flat, non-fragile sections, which were clamped by plastic jaws (Figure 1). The jaws were either square (for a fixed constraint) or wedge shaped (for a free constraint). These standard supports allow for easily comparable results, although the results will not accurately reflect the final performance. For other geometries (for example a disk structure tested) temporary support points were attached to the shaker table using double-sided tape, which has entirely satisfactory structural performance at the frequencies and amplitudes studied.

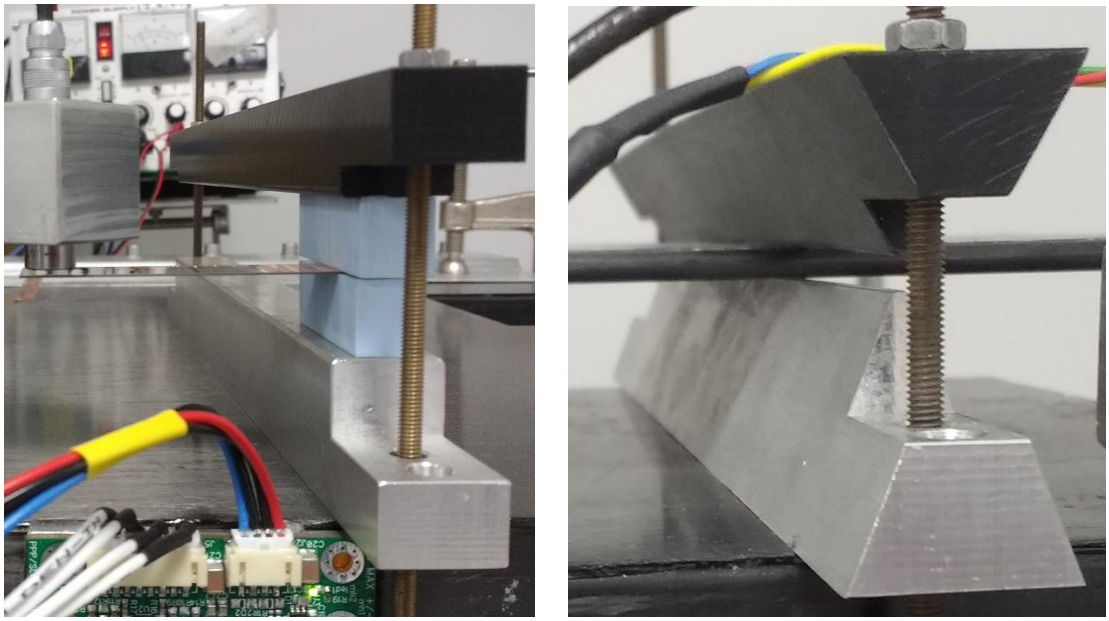

Figure 1: Clamp to constrain ladder structures on the shaker table: Fixed (left) and free (right) constraints. The left picture also shows a displacement sensor (above the ladder to the left), and the board which holds the accelerometer and its amplifier (on the bottom).

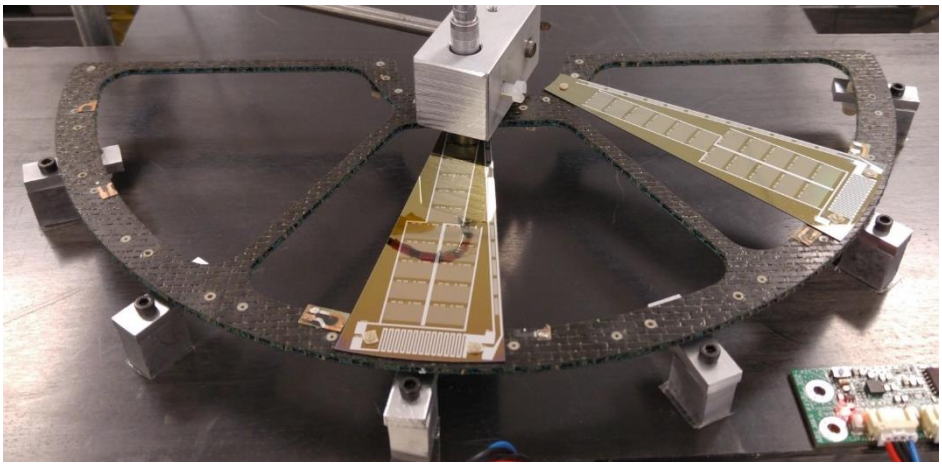

Figure 2: Support of a disk structure for DEPFET from Valencia on the vibration shaker table. The supports are small aluminium blocks attached to the table by double-sided tape.

Another aspect required for the characterization of support structures is the damping, characterized by the quality factor (Q factor)[1]. This will be significantly influenced by non-rigid connections (in particular service connections). Again, for the prototypes tested such connections were absent due to the level of maturity of the prototypes, and for a better prediction of final performance these connections would have to be prototyped as well.

An overview over the data produced by a standard run can be found in the appendix.

2.1.3. Future plans

One limitation in our setup is the dynamic range of the AWG. While it is already 14 bit, a larger dynamic range would be helpful to allow maintaining a large table displacement at frequencies at the edge of our standard frequency range (below 5 Hz and at frequencies above 200 Hz). Recently we have started to use a 100-step digital potentiometer to increase this range. Another application for this type of component we want to investigate in the future is for the synchronization of the amplitudes of two drive motors, one at each end of the shaker table, which should help to reduce rocking modes of the table.

Another interesting development is the study of small spherical glass retroreflectors (down to a diameter of 1 mm), which we are investigating for a different project, for the use with our frequency scanning interferometry (FSI) system. If these retroreflectors can provide sufficient light output, this would give us a way to access this very precise, long-distance non-contact displacement measurement system, either alongside or replacing the capacitive sensor system. The retroreflectors we currently have to use with this system are bulky and would add considerable weight to the structure. The novel retroreflectors would weigh about 10 mg and therefore have little effect on the dynamic behaviour of the structures.

[1] A higher Q factor corresponds to less damping, and leads to a sharper resonance peak in the frequency response.

AIR FLOW SETUP

2.1.4. Setup description

As discussed above, prediction of position stability in air flow is difficult. A first indication of the performance can be gained from the knowledge of resonance frequencies and Q factors obtained from the vibration tests. To further allow for comparative studies for different structures we have built an air flow wind channel. As air flow cooling is currently considered for vertex systems for future electron colliders the dimension of our test wind channel is small (25×60 mm^2). The air flows used for testing are a few m/s. Laminar flow is achieved by a long square section in front of the test region. However, in practice turbulent flow around the structure under test is unavoidable due to the small dimensions.

Displacement measurements using capacitive sensors is not practical, because they have to be brought close (within < 1 mm) to the surface of the structure, which would affect the air flow around the structures. It is therefore measured with a reflective light sensor (Keyence LK-081), which is less accurate (slightly better than 1 µm), but the sensor can be placed well outside of the test channel, with a small slot in the channel ceiling to provide passage for the laser beam.

2.1.5. Supports

As for any structural study the ideal support interface for the structures under test would be the final design. However, such interfaces have not been available for the air flow test performed so far, and we have again constructed a clamp system (Figure 3) which allows for flexible use for different structure geometries to provide comparability. Additionally, this support must be stiff, while its shape and dimension should minimize impact on the air flow.

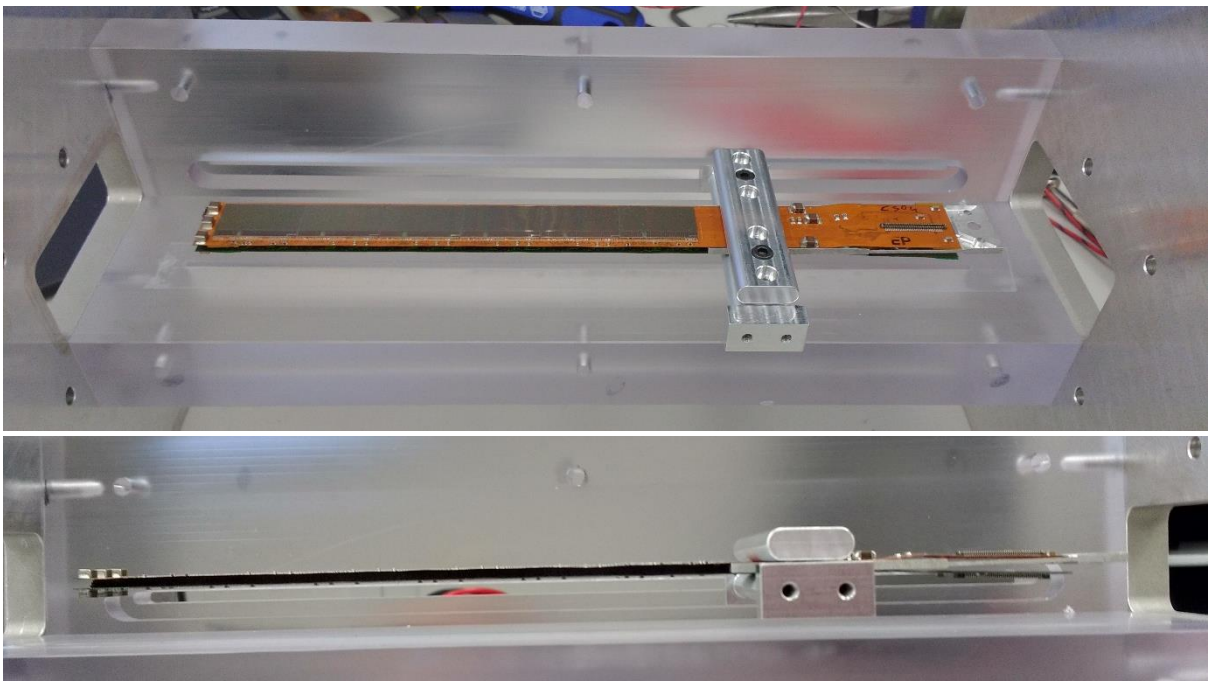

Figure 3: Opened test channel and ladder support with a PLUME ladder from Bristol University (side views). Air flow is from the left to minimize disturbance by the support.

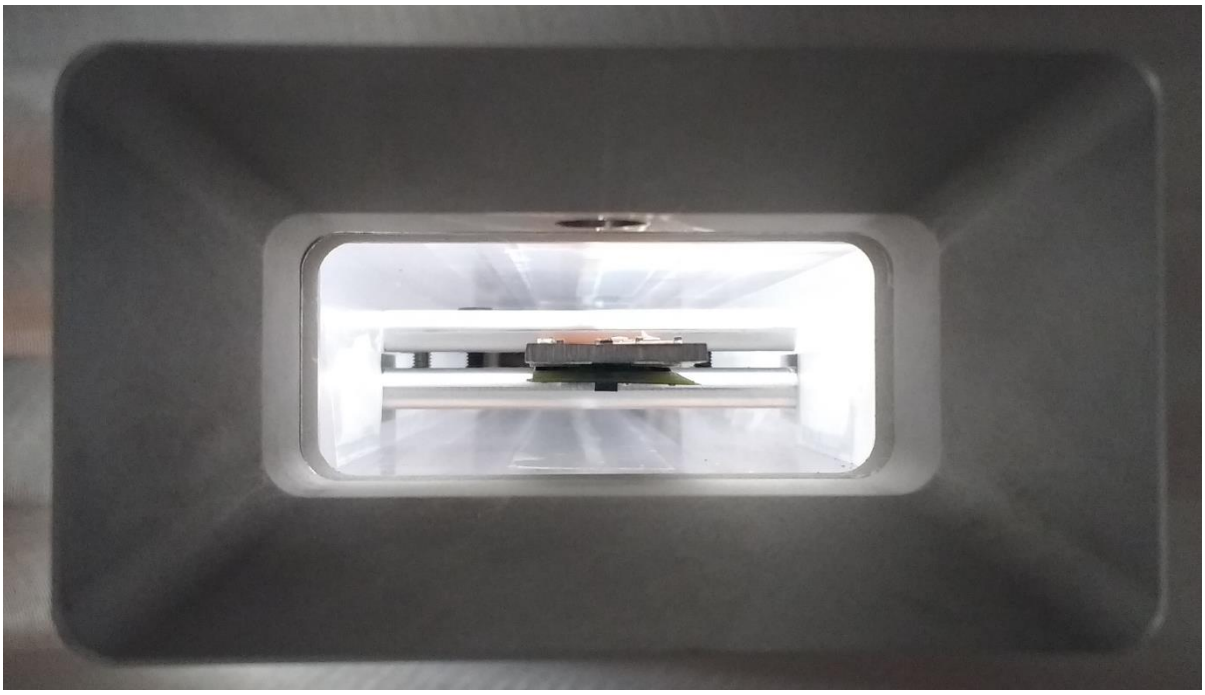

Figure 4: Test channel end view.

2.1.6. Future plans

Measurements so far have been done with room temperature air flow. Recently, we have added a large heat exchanger box to reduce the air temperature in exchange with a chilled water system, but we have not been able to fully operate this system before the publication of this report.

Again of interest will be the development of small spherical retro reflectors to allow for the use of FSI, which would provide a significant improvement of accuracy over the reflective laser sensor. Due to the higher channel count in the FSI system this could also allow for mode shape analysis under air flow.

2.2. THERMAL STUDIES

The main difficulty for deformation studies under thermal loads is the need to provide a stable base for the sensors, against which the deformations can be measured. In particular, this becomes challenging if the temperature variations involve changes of the environment temperature. Here the FSI system could be very helpful, but our system currently is limited to four lines of sight, although it can be upgraded easily, we have therefore not used it yet for such studies.

However, we have been able to use the system for the less ambitious task of measuring coefficients of thermal expansions (CTEs), to confirm material properties used for the design of tracker studies (carbon fibre and plastic). With the current retroreflectors the issue is to support one end of the specimen in a way that allows free movement. For high-strength specimens we hang the setup vertically to let the free end move freely. Where the sample is not strong enough for such a loading the setup is used vertically, with the free end supported by steel balls. The temperature (and humidity) is varied inside a thermal chamber.

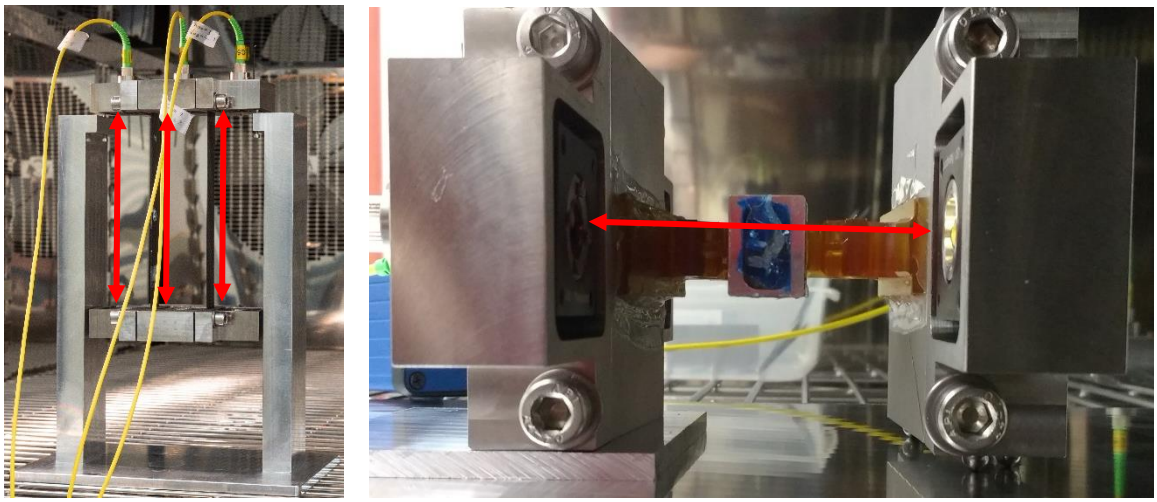

Figure 5: CTE measurements using FSI. Vertical (left) and horizontal (right) orientation. FSI lines of sight are indicated by red arrows.

3. TEST PROCEDURES

3.1. VIBRATION

There are two types of vibration tests we have been performing at the facility: Frequency scans and broadband excitations. In a frequency scan the system is excited with a sine wave of fixed frequency. The amplitude is adjusted until a defined level is achieved, typically characterized by a target acceleration of the shaker table, although a target displacement can be selected as well. This adjustment is necessary as the system (function generator, amplifier, motor and table) is not linear and its exact characteristics does depend on the load and support of the structure under test). The response at this frequency is measured and the system proceeds to the next frequency, until the scan is completed. The system records the excitation amplitude needed to achieve the requested table response (acceleration or displacement), which then can be used as a calibration for further data taking.

At the same time, the system records the displacement response of the structure, resulting in a full structure response spectrum that can be used to identify spectral features like resonance frequencies and Q factors, but also as a whole for convolution with an ideal or measured ASD function.

Typical acceleration levels used are between $10^{-6}\ g^2$/Hz and $10^{-5}\ g^2$/Hz, and displacements are typically 1 μm or smaller. The frequency range studied is typically between 5 and 500 Hz. The lower limit is given by the power that the amplifier can supply to the motor. Lower frequencies are of little interest as they correspond to wavelengths of several hundreds of meters, and result in coherent movements of all components in the tracker, which do not affect the alignment. The upper frequency limit has been chosen to cover several resonances even for relatively stiff structures, although in practice, the displacement response has, at these frequencies, dropped to levels which are indistinguishable from noise with the current instrumentation (10 nm and below).

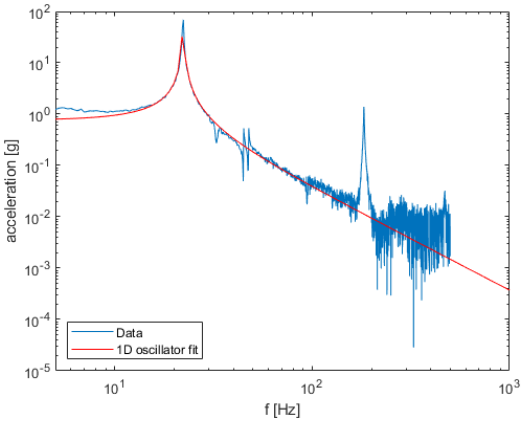

Figure 6: Acceleration response for a 1.2 m ATLAS stave. The blue line shows the measured data, the red line is the response of a simple damped 1D harmonic oscillator, fitted to the data. The fit yields a result for the first mode frequency and its Q factor.

In broadband excitations the user can set a uniform acceleration level between two frequencies. In practice, we have mostly used a uniform ASD between 5 and 500 Hz, the standard frequency range. This test makes use of the calibration taken in the frequency range to achieve the uniform response. In principle it should also be possible to employ a user-supplied ASD spectrum, which could, for example, be obtained from a vibration level measurement at the location of the experiment the structure is intended for.

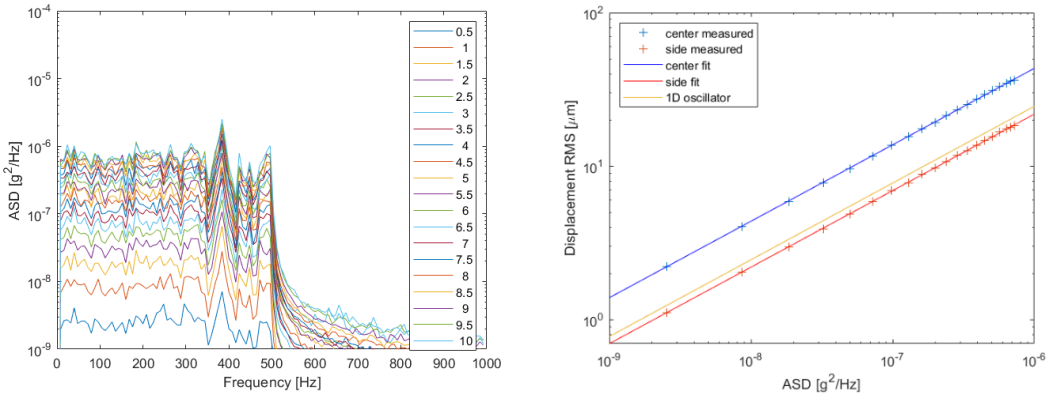

Figure 7: Left: Broadband excitation spectra (5 to 500 Hz selected) for different average acceleration levels. Right: RMS displacement at two points on a 1.2 m ATLAS stave in response to broadband excitation as a function of average ASD. The orange curve shows expectations for a simple damped 1D oscillator (Miles' equation [2]).

3.2. AIR FLOW

For a given air flow, an average displacement spectrum can be obtained from the Fourier transform of the displacement signal. The observed spectra will reflect the structure response function as can be seen in Figure 8, which shows displacement spectra for a PLUME detector ladder. The peak at slightly more than 50 Hz is consistent with the frequency of the first mode found on the vibration table (at 51.6 Hz). The slight shift in the resonance frequency is likely to be caused by a different length of the unsupported part of the ladder. The peak at 40 Hz appears to be a contribution of the air flow setup, which needs further investigation and correction.

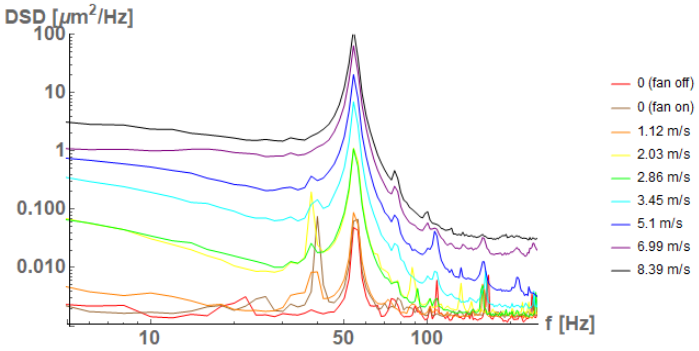

Figure 8: Spectral displacement response for different air flows for a PLUME vertex detector ladder.

A simple overall benchmark number for the performance of the structure in air flow is the RMS displacement over an extended period (Figure 9).

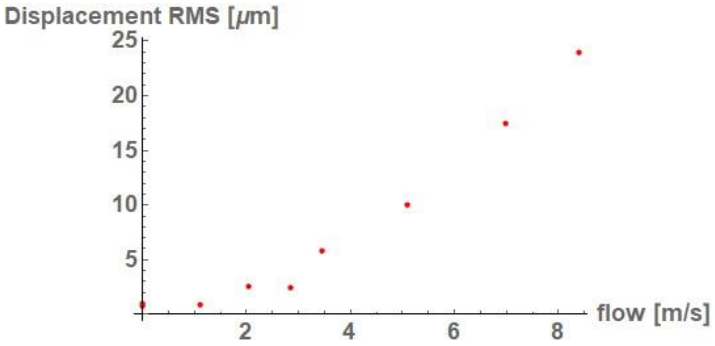

Figure 9: Displacement RMS as a function of air flow for a PLUME vertex detector ladder.

4. PERFORMANCE EXTRAPOLATION

The measurements described in this report can be immediately useful for assessing the performance of a given design when the directly measured RMS displacement is used. The importance of the support interface for the quality of these results has already been referred to throughout this report.

The results become even more useful if they allow extrapolation to different load conditions. This is most easily done in the case of external vibrations, where the structure response can be used to predict performance for a given vibration ASD by multiplication of the spectra. On an even simpler level, a quick estimate for a given constant ASD, can be obtained from Miles' equation [2], which is an expression strictly derived for a simple damped 1D oscillator, but gives reasonable predictions for more complex dynamic systems.

More challenging is the extrapolation of the displacement data in air flow. To our knowledge no simple model to parametrize this effect exists. However, we will investigate the possibility of such models when we have more data in our setup, potentially combining approaches to the treatment of external vibrations.

The situation for thermo-mechanical deformations is slightly better. In principle, if the thermal environment and conditions of the systems are known it is possible to predict the response of a structure using finite element analysis (FEA). Measurements of the type performed in our facility can support the understanding of the structural properties underlying these predictions.

5. APPENDIX: OUTPUT DATA FORMATS

5.1. FREQUENCY SCAN

Four .csv files are generated for each run.

5.1.1. Scan *xxx*.dat[2]

This file contains the amplitude (column 2n-1) and phase (column 2n) for a sinusoidal fit to the data for each sensor channel for each frequency in the scan. The frequency in the fit is fixed to the generated frequency. Data is in V measured by the ADC. Conversion factors are listed below.

n	Data	Conversion
1	Frequency [Hz] (phase not used)	-
2	1st accelerometer z	1/0.660 g/V
3	1st accelerometer x	1/0.660 g/V
4	1st accelerometer y	1/0.660 g/V
5	2nd accelerometer z	1/0.660 g/V
6	2nd accelerometer x	1/0.660 g/V
7	2nd accelerometer y	1/0.660 g/V
8	Excitation (function generator)	1 V/V
9	Laser displacement sensor	3000 µm/V
10	Capacitive sensor 1	100 µm/V
11	Capacitive sensor 2	100 µm/V
12	Capacitive sensor 3	100 µm/V
13	Capacitive sensor 4	100 µm/V
14-17	Not connected	

5.1.2. Laserdisp *xxx*.dat

Data from the displacement sensors for each frequency in the scan

Column	1	2	3	4	5	6	7	8 to 16
		Laser sensor			Capacitive sensor 1			Repeat for capacitive sensors 2-4[3]
Data	Frequency [Hz]	Average [µm]	RMS [µm]	RMS at excitation [µm]	Average [µm]	RMS [µm]	RMS at excitation [µm]	

[2] *xxx* here stands for the date and time of the start of data taking for this run.

[3] Data for four more channels are stored, but these are currently not connected.

Average: this give the displacement measurement for this frequency value (small variations due to movements of the speaker membrane)
RMS: RMS of all data at this frequency
RMS at excitation: RMS of sinusoidal fit to the sensor data with the frequency constrained to the generated frequency.

5.1.3. Noise *xxx*.dat

Average spectral density data of data recorded for frequencies, which are not currently excited ($f < f_{excitation}/2$ or $f > 2f_{excitation}$). The shaker table is excited at the frequencies as for the other outputs, but the spectra are averaged excluding a frequency window around the excitation frequency, in this way giving a realistic estimate of the background vibration levels. This allows assessment of noise spectra for different sensors.

Line	
1	List of frequencies [Hz]
2	1st accelerometer z ASD [g^2/Hz]
3	1st accelerometer x ASD [g^2/Hz]
4	1st accelerometer y ASD [g^2/Hz]
5	2nd accelerometer z ASD [g^2/Hz]
6	2nd accelerometer x ASD [g^2/Hz]
7	2nd accelerometer y ASD [g^2/Hz]
8	Excitation (function generator) (uncalibrated)
9	Laser displacement [μm^2/Hz]
10	Capacitive sensor 1 [μm^2/Hz]
11	Capacitive sensor 2 [μm^2/Hz]
12	Capacitive sensor 3 [μm^2/Hz]
13	Capacitive sensor 4 [μm^2/Hz]
14-17	Not connected

5.1.4. Scale *xxx*.dat

Data describing the excitation amplitude for each frequency. This file can be used to create a calibration file of the excitation amplitude as function of the frequency.

Column	1	2	3	4	5	6
	Frequency [Hz]	Amplitude [V]	Acceleration amplitude measured at excitation frequency squared [g^2]	Number of iterations needed to reach requested acceleration amplitude	Last step size used in reaching requested acceleration amplitude [V]	Power supplied to speaker [W]

Data in column 3 can be either one of the two accelerometers or the average of the two (selected at run time).
Data in columns 4 and 5 are only interesting if amplitude is adjusted during scan (not constant or obtained from data file).

5.2. AIR FLOW MEASUREMENTS

There is one output .csv file. This file contains data from the laser triangulation sensor in µm. It contains first the data for 1000 events (one per row) and then in the last row the combined data for all 1000 events. The header contains the information of the air flow and the sampling rate and number of samples.
For the data per event the first column contains the average of all displacements sampled in an event, the second column the RMS of these data and the remainder the DSD coefficients for this event (the number of coefficients equals the number of samples divided by 2) in units of $\mu m^2/s$. The frequencies corresponding to the coefficients can be found from (f_sampling/n_samples)*i.
The last line contains in the first column the average of all displacements sampled in all 1000 events (1000*number of samples datapoints) and the second column the RMS of all these data. The remainder gives the average of the FFT coefficients from the 1000 events.

REFERENCES

[1] G.Viehhauser, Thermal management and mechanical structures for silicon detector systems, 2015 *JINST* **10** P09001.

[2] J.W.Miles, On Structural Fatigue Under Random Loading, Journal of the Aeronautical Sciences, pg. 753, November, 1954.